Monte Carlo Simulation for Vapor-Liquid Equilibrium of Binary Mixtures CO₂/CH₃OH, CO₂/C₂H₅OH, and CO₂/CH₃CH₂CH₂OH

Sung Doo Moon

Department of Chemistry, Pukyong National University, Busan 608-737, Korea

Gibbs ensemble Monte Carlo simulations were performed to calculate the vapor-liquid coexistence properties for the binary mixtures CO₂/CH₃OH, CO₂/C₂H₅OH, and CO₂/CH₃CH₂CH₂OH. The configurational bias Monte Carlo method was used in the simulation of alcohol. Density of the mixture, composition of the mixture, the pressure-composition diagram, and the radial distribution function were calculated at vapor-liquid equilibrium. The composition and the density of both vapor and liquid from simulation agree considerably well with the experimental values over a wide range of pressures. The radial distribution functions in the liquid mixtures show that CO_2 molecules interact more strongly with methyl group than methylene group of C_2H_5OH and $CH_3CH_2CH_2OH$ due to the steric effects of the alcohol molecules.

Keywords : Monte Carlo simulation, Carbon dioxide, Alcohol.

Introduction

There has been much progress in the development of Monte Carlo simulations. Frankel[1] *et al.* developed the configurational bias Monte Carlo (CBMC) method for the simulation of chain molecules in dense systems. In this simulation, the entire molecule dose not move at random, but the chain molecule is grown segment by segment in such a way that regions of favorable energy are found. Pablo[2] *et al.* proposed the continuum configurational bias (CCB) Monte Carlo method, which is similar to the CBMC method. These methods have improved the efficiency of simulations compared with conventional Monte Carlo simulations. The Gibbs ensemble Monte Carlo (GEMC) simulation[3] enables us to calculate the phase equilibrium of pure components and mixtures, and is more convenient than the indirect method involving computations of chemical potential. Because the probability of the successful insertion of a chain molecule into a high density system in simulation is very low, a combination of the GEMC simulation with the CBMC method has been used recently. For example this method applied to calculate the phase equilibrium of *n*-alkanes,[4] branched alkanes,[5] alkanols,[6] *n*-alkanes mixture,[7] CO₂/perfluoroalkane mixture,[8] and methanethiol/C₃H₈ mixture.[9] However, the successful insertion of a molecule is difficult for larger molecules such as heavy hydrocarbons, even if the CBMC method are used. Several techniques have been reported in order to increase the probability of the successful insertion. For example, Camp and Allen[10] introduced the pseudo-Gibbs ensemble technique which no longer employs molecule transfer moves; instead, the volumes of the two simulation boxes are altered to mimic molecule transfer.

CO₂ is nontoxic, nonflammable, relatively inexpensive, and its critical temperature is low. Supercritical CO₂ has been used as an extraction solvent in many industries. Several actual or commercial applications[11] include extraction of fragrances and flavors from liquids, deodorization of oils, extraction of oil seeds, fractionation of highly unsaturated methyl esters derived from fish oil triglycerides, separation of organic materials from water, decaffeination of green coffee, removal of cholesterol from butter, removal of cocoa butter from cocoa beans, and extraction of hops, spices, and nicotine from raw materials. The extraction efficiency of supercritical CO₂ can be improved with the addition of cosolvents.

In this study the GEMC methods were performed to calculate the vapor-liquid coexistence properties for CO₂ mixtures with CH₃OH, C₂H₅OH, and CH₃CH₂CH₂OH. In the following sections the details of the molecular model and the simulation method are described. Thereafter, the simulation results are presented and discussed.

Molecular Model and Simulation Method

The CO₂ molecule[12] was assumed to be composed of two sites connected by a rigid length of 0.237 nm for the reasons of simplicity. For the alcohol molecules, CH₃ and CH₂ groups were considered as single interaction sites, and bond lengths and bond angles were fixed in simulations. The geometry of the alcohol molecules[6,13] were adopted as follows: r (H-O) = 0.0945 nm, r (O-C) = 0.143 nm, r (C-C) = 0.153 nm, $\angle$ HOC = 108.5°, $\angle$ OCC = 108°, and $\angle$ CCC = 112°. The interaction between molecule k and l was calculated by Coulombic and Lennard-Jones (LJ) potentials.

$$u_{kl} = \sum_{ij} \left(\frac{q_i q_j e^2}{r_{ij}} + 4\varepsilon_{ij} \left[\left(\frac{\sigma_{ij}}{r_{ij}} \right)^{12} - \left(\frac{\sigma_{ij}}{r_{ij}} \right)^{6} \right] \right) \tag{1}$$

where r_{ij} is the distance between site i on molecule k and site j on molecule l. q_i is a partial charge located at site i, and e denotes the electronic charge. ε_{ij} and σ_{ij} were obtained using the modified Lorentz-Berthelot rules given by

Table 1. Parameter values[6,13] for the sites on the alcohol molecules. Sites in parentheses denote neighbouring sites, and k is Boltzmann constant. CH_n denotes CH_2 or CH_3

Site	σ (nm)	ε/k (K)	q (e)
H(O)	0.	0.	0.435
(H)O	0.307	85.55	-0.700
(HO)CH$_2$(CH$_n$)	0.3905	59.38	0.265
(CH$_2$)CH$_2$(CH$_n$)	0.3905	59.38	0.
(HO)CH$_3$	0.3775	104.17	0.265
(CH$_2$)CH$_3$	0.3905	88.06	0.

$$\sigma_{ij} = 0.5(\sigma_i + \sigma_j) \tag{2}$$

$$\varepsilon_{ij} = (1-\delta_{ij})(\varepsilon_i\varepsilon_j)^{0.5} \tag{3}$$

where ε_i and σ_i are the LJ parameters for site i, and δ_{ij} is the inter-site interaction parameter which modifies the well depth for the interaction of unlike sites. The LJ parameters and the partial charges of sites on the alcohol molecules are summarized in Table 1. For each site of CO_2, the value $\sigma = 0.2989$ nm was taken from the 2CLJ model,[12] and the value[14] of ε/k for CO_2 was assumed to be 150.512 K. The potential between CO_2 molecules calculated with these values of ε and σ includes the contribution of potential arising from the quadrupole-quadrupole interaction between CO_2 molecules.

In addition to LJ and Coulombic interaction, the torsional energy of molecule with more than three sites was taken into account as in the following equation.

$$u_t(\phi) = 0.5\,V_1(1+\cos\phi) + 0.5\,V_2(1-\cos2\phi) \\ + 0.5\,V_3(1+\cos3\phi) \tag{4}$$

where ϕ is the dihedral angle and $u_t(\phi)$ is the torsional energy. The Fourier coefficients V_i are listed in Table 2.

Simulation Method. The GEMC[3] and the CBMC method[15] were carried out using conventional procedures in principle. All simulations were performed for a total of 512 molecules in the two cubic simulation boxes I and II, and three dimensional periodic boundary conditions were used. The types of Monte Carlo moves were as follows: (a) molecule translation, (b) molecule rotation, (c) CBMC conformational change, (d) volume rearrangement in the NPT ensemble, and (e) molecule transfer. Move (a), (b), and (d) were carried out by means of the procedures in ref. 14.

In move (c), a alcohol molecule was selected at random, and whether to regrow toward the head or the tail was chosen randomly. Then the alcohol molecule was cut at a randomly selected segment, and regrowing began at the randomly selected segment. The number of trial orientations was fixed at 6. Move (c) was accepted with the probability[15]

Table 2. Fourier coefficients[6] V_i (kJ/mol) for the torsional energy in Eq. (4). CH_n denotes CH_2 or CH_3

Torsion axis	V_1	V_2	V_3
(CH$_n$)-CH$_2$-CH$_2$-(OH)	2.937	-0.887	12.803
(CH$_n$)-CH$_2$-O-(H)	3.489	-0.485	3.125

$$P_c = \min\left[1, \frac{W_n}{W_o}\right] \tag{5}$$

where W_o and W_n are the Rosenbluth factors of old and new configuration, respectively. In move (e), it was first decided at random to choose box I or II for trial creation. Then the type of molecule to be transferred was chosen at random. For a transfer of CO_2 molecule from box II to I, the trial move was accepted with a probability given by[3]

$$P_t(1) = \\ \min\left[1, \exp\left(-\beta\left[\Delta E^{\mathrm{I}} + \Delta E^{\mathrm{II}} + kT\ln\frac{V^{\mathrm{II}}(N_1^{\mathrm{I}}+1)}{V^{\mathrm{I}}N_1^{\mathrm{II}}}\right]\right)\right] \tag{6}$$

where ΔE^{I} is the energy change for the trial move in box I, V^{I} is the volume of box I, N_1^{I} is the number of CO_2 molecules in box I, and β is $1/kT$. Here k is Boltzmann constant, and T is temperature. For a transfer of alcohol molecule from box II to I, the trial move was accepted with a probability given by[4,16]

$$P_t(2) = \min\left[1, \frac{N_2^{\mathrm{II}}V^{\mathrm{I}}W_n}{(N_2^{\mathrm{I}}+1)V^{\mathrm{II}}W_o}\right] \tag{7}$$

where N_2^{I} is the number of alcohol molecules in box I. If box II is chosen for the creation, the superscripts I and II in Eq. (6) and Eq. (7) are interchanged.

Each configuration in simulations was generated by a randomly selected Monte Carlo move. The five types of Monte Carlo moves occurred with the following probabilities: 20%, 20%, 20%, 10%, and 30% for move (a), (b), (c), (d), and (e), respectively. For move (a), (b), and (d), the maximum move was adjusted to give an average acceptance ratio of 40% every 25000 configurations.

For the LJ part of the potential, the interactions were truncated if the inter-site distance was larger than cutoff distance, which was half the length of the simulation box. The ranges of cutoff distance were 1.55-7.04 nm for the vapor phase and 1.24-1.58 nm for the liquid phase in this study. The corrections to the potential arising from truncations of inter-site interactions were calculated according to[9]

$$E_{cut} = 2\frac{\pi}{V}\sum_k^M\sum_l^M\sum_i^{\text{on }M_k}\sum_j^{\text{on }M_l}\int_{r_c}^\infty N_kN_lr_{ij}^2g_{ij}(r)u_{ij}(r)dr \tag{8}$$

where M is the number of different components in the solution, V is the volume of the simulation box. M_k and M_l are the number of sites on molecule k and l, respectively. The radial distribution functions (RDFs) $g_{ij}(r)$ are taken to be 1 beyond the cutoff distance r_c, and $u_{ij}(r)$ is the LJ potential for the site i and j. The Ewald sum for Coulombic terms was carried out by using the program code[17] MDMPOL. The initial configurations were obtained by putting 256 molecules on a face-centered cubic lattice in each of the simulation boxes. The initial densities were taken as 0.1 g/cm^3 for the vapor phase and were taken as 0.8 g/cm^3 for liquid phase. The simulation results were almost not affected by

the initial densities. However, the initial compositions were chosen to be approximately the experimental compositions of the vapor and the liquid phases for fast equilibration.

The number of configurations generated in equilibration run was 1×10^6, and that in equilibrium run was 2×10^6. The simulation run was divided into many blocks, each of which consists of 25000 configurations. The properties of system were calculated by accumulating the properties every 50 configurations and by averaging them. The estimated errors for properties were obtained by calculating the standard deviation of the block average properties.

Results and Discussion

Estimating the value of δ_{ij} is difficult because thermodynamic properties are significantly sensitive to the interaction potentials. For interactions between CO_2 and alcohol,

the values of δ_{ij} were set at -0.1, -0.05, and 0 for CO_2-CH_3OH, CO_2-C_2H_5OH, and CO_2-$CH_3CH_2CH_2OH$, respectively.

Table 3 shows the simulation results for some mixtures along with the experimental ones. The torsional energies of the C_2H_5OH and $CH_3CH_2CH_2OH$ are about 3 and 10 kJ/mol, respectively, and are almost independent of pressure, temperature, and mole fraction of alcohols (not shown in the Table 3). On the other hand, to test the effects of larger simulations run on the calculated results, the densities were calculated for 2×10^6 and 3×10^6 configurations in equilibration run and equilibrium run, respectively. The vapor and liquid densities of the mixture CO_2/CH_3OH at 290 K and 4.826 MPa were 0.137 and 0.852 g/cm³, those of the mixture CO_2/C_2H_5OH at 303.12 K and 2.43 MPa were 0.048 and 0.821 g/cm³, those of the mixture $CO_2/CH_3CH_2CH_2OH$ at 313.4 K and 2.6 MPa were 0.049 and 0.844 g/cm³, respec-
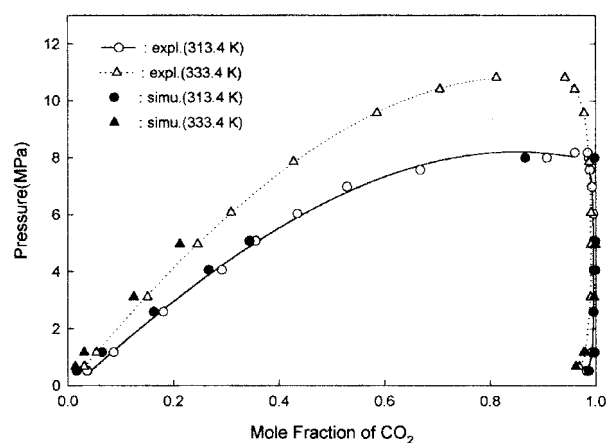
Table 3. Simulation results[a] for the binary mixtures $CO_2(1)$/alcohol(2). P denotes the pressure, y_1 the mole fraction of CO_2 in the vapor, x_1 the mole fraction of CO_2 in the liquid, ρ the density, and E the total energy which is represented by a sum of the LJ, Coulombic, and torsional energies. Subscripts V and L refer to the vapor and the liquid phase, respectively

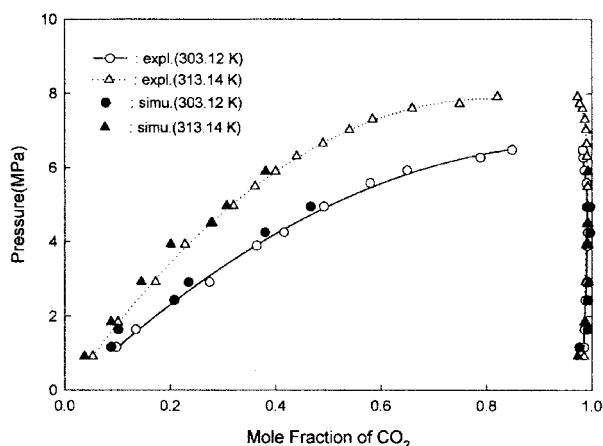| P (MPa)	y_1 expl.[b]	y_1 simu.	x_1 expl.[b]	x_1 simu.	ρ_V (g/cm³)	ρ_L (g/cm³)	$-E_V$ (kJ/mol)	$-E_L$ (kJ/mol)
mixture CO_2/CH_3OH at 290 K
1.379	0.991	0.931(20)	0.116	0.121(15)	0.028(2)	0.787(15)	0.909(127)	32.4(5)
2.758	0.995	0.961(5)	0.248	0.270(24)	0.062(5)	0.832(18)	1.60(12)	29.1(6)
4.826	0.996	0.976(6)	0.667	0.644(19)	0.136(10)	0.860(24)	2.35(21)	18.7(6)
mixture CO_2/C_2H_5OH at 303.12 K
1.16	0.985	0.976(5)	0.098	0.088(8)	0.022(1)	0.805(9)	0.339(88)	41.1(5)
1.64	0.986	0.992(8)	0.135	0.102(9)	0.031(2)	0.803(9)	0.420(73)	40.7(4)
2.43	0.988	0.993(6)	0.208	0.208(10)	0.048(4)	0.817(10)	0.654(90)	36.7(6)
2.91	0.990	0.993(5)	0.275	0.235(11)	0.060(5)	0.826(8)	0.790(92)	35.9(5)
4.25	0.992	0.997(3)	0.416	0.379(10)	0.098(8)	0.845(13)	1.30(14)	30.5(5)
4.95	0.991	0.997(3)	0.492	0.467(10)	0.121(13)	0.853(14)	1.59(21)	27.8(5)
mixture CO_2/C_2H_5OH at 313.14 K
0.91	0.985	0.973(11)	0.053	0.037(12)	0.016(1)	0.792(9)	0.251(67)	42.2(6)
1.84	0.986	0.988(8)	0.101	0.088(12)	0.034(2)	0.795(12)	0.461(80)	40.0(7)
2.92	0.988	0.994(4)	0.172	0.145(11)	0.057(4)	0.803(10)	0.751(91)	38.5(7)
3.93	0.989	0.993(3)	0.228	0.201(8)	0.082(7)	0.808(10)	1.07(12)	36.5(5)
4.50	0.991	0.993(5)	0.280	0.277(15)	0.099(9)	0.821(9)	1.28(15)	33.7(5)
4.97	0.991	0.991(5)	0.320	0.307(10)	0.110(9)	0.828(12)	1.46(19)	32.6(7)
5.90	0.992	0.993(5)	0.400	0.381(11)	0.146(13)	0.832(12)	1.90(20)	29.8(7)
mixture $CO_2/CH_3CH_2CH_2OH$ at 313.4 K
0.518	0.983	0.987(3)	0.037	0.017(5)	0.009(1)	0.830(6)	0.125(33)	51.0(6)
1.171	0.993	0.998(2)	0.087	0.065(12)	0.021(1)	0.827(7)	0.274(45)	48.5(6)
2.600	0.996	0.995(4)	0.181	0.163(8)	0.050(3)	0.846(8)	0.651(85)	44.9(6)
4.062	0.996	0.999(2)	0.292	0.267(10)	0.085(7)	0.853(10)	1.11(13)	40(1)
5.076	0.996	0.999(1)	0.356	0.344(13)	0.115(11)	0.859(12)	1.48(19)	37(1)
7.999	0.987	0.998(2)	0.908	0.867(6)	0.272(30)	0.805(30)	3.39(36)	13.5(4)
mixture $CO_2/CH_3CH_2CH_2OH$ at 333.4 K
0.668	0.969	0.962(3)	0.031	0.014(5)	0.011(1)	0.817(7)	0.171(47)	50.2(5)
1.163	0.980	0.977(4)	0.054	0.031(6)	0.019(1)	0.822(9)	0.272(57)	49.2(7)
3.118	0.990	0.997(1)	0.151	0.125(6)	0.056(4)	0.829(8)	0.699(85)	45.4(5)
4.966	0.991	0.999(1)	0.246	0.212(21)	0.098(8)	0.835(10)	1.20(13)	41(1)

[a]The numbers in parentheses give the accuracy of the last digit. [b]The experimental data were obtained from ref. 18, ref. 19, and ref. 20 for mixtures CO_2/CH_3OH , CO_2/C_2H_5OH, and $CO_2/CH_3CH_2CH_2OH$, respectively.
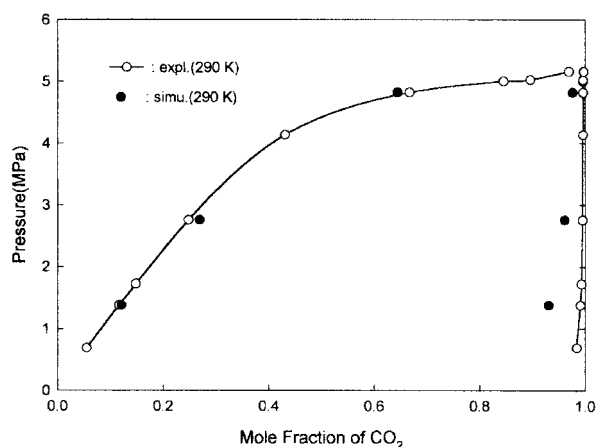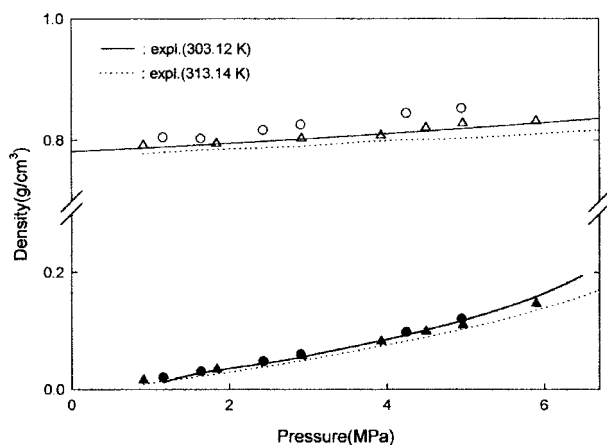
Figure 1. The pressure-composition diagram for the binary mixtures CO_2/CH_3OH. Experimental data were taken from ref. 18.

Figure 2. The pressure-composition diagram for the binary mixtures CO_2/C_2H_5OH. Experimental data were taken from ref. 19.

Figure 3. The pressure-composition diagram for the binary mixtures $CO_2/CH_3CH_2CH_2OH$. Experimental data were taken from ref. 20.

Figure 4. Simulated densities of the vapor and the liquid for the mixtures CO_2/C_2H_5OH at 303.12 K (●, ○) and 313.14 K (▲, △). Experimental data were taken from ref. 19.
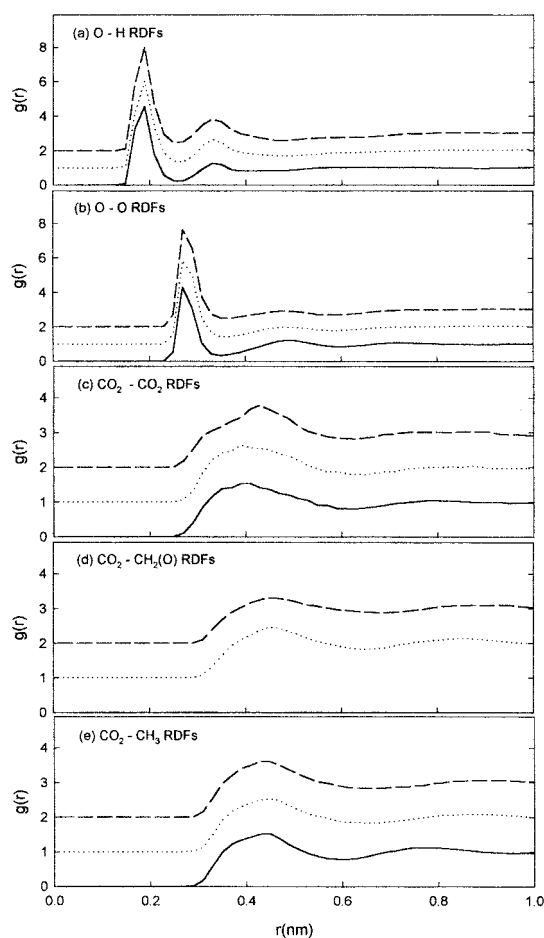
tively. These values are very similar to the simulation results of the corresponding mixture in Table 3, indicating that the configurations 1×10^6 and 2×10^6 are large enough for equilibration and equilibrium, respectively.

Figures 1, 2, and 3 show the pressure-composition diagram for the binary mixtures CO_2/CH_3OH, CO_2/C_2H_5OH, and $CO_2/CH_3CH_2CH_2OH$, respectively. The calculated mole fractions of CO_2 in the mixtures CO_2/C_2H_5OH and $CO_2/CH_3CH_2CH_2OH$ agree considerably well with the experimental values over a wide range of pressure. However, the mole fractions of CO_2 in the vapor mixture CO_2/CH_3OH deviate considerably from the experimental values, especially at low pressure. The largest deviation is from the vapor mixture at 290 K and 1.379 MPa, where the mole fraction of CO_2 is about 6.1% smaller than the experimental value.

The experimental densities and the calculated densities of the mixture CO_2/C_2H_5OH at vapor-liquid equilibrium are shown in Figure 4. The simulation results agree fairly well with the experimental ones. The experimental vapor-liquid coexistence densities of the mixtures CO_2/CH_3OH and $CO_2/CH_3CH_2CH_2OH$ with which to compare the coexistence densities from simulation have not been found.

RDFs are important in understanding of the structures of fluids. RDFs $g_{xy}(r)$ gives the probability of finding a site of type y at a distance r from a site of type x. Experimental information about RDFs can be obtained by neutron scattering and x-ray diffraction. Nevertheless, due to the many scattering centers in bulk liquids, the output from scattering and diffraction experiments are difficult to analyse.[21] Figure 5 shows the RDFs in the liquid mixtures calculated from Monte Carlo simulation. Because the angular distributions were not calculated in this study, the orientational informations were not given in the RDFs. In Figure 5(a) and 5(b), the first sharp peaks of the O-H and the O-O RDFs clearly reflect the hydrogen bonding. The second peak of O-H RDFs is due to the hydrogen bonding formed indirectly. The first two peaks of the O-H and the O-O RDFs are nearly located at 0.19 and 0.33 nm for O-H, and 0.27 and 0.48 nm for O-O. The positions of these peaks are very similar to the ones found for pure alcohols.[13,22]

The coordination number, which indicates the average number of the first neighbours for a given site, was calculated by
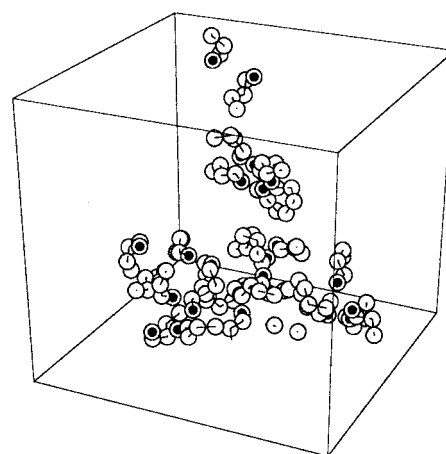
Figure 6. Snap shot for the configuration of the liquid mixture $CO_2/CH_3CH_2CH_2OH$ with mole fraction of $CH_3CH_2CH_2OH$ = 0.133 at 313.4 K and 7.999 MPa. ⊙ : hydrogen atom, ○ : oxygen atom or CH_n group. All CO_2 molecules were omitted for clarity.

MPa and those for pure liquid $CH_3CH_2CH_2OH$ are not large. These probably result from clustering between alcohol molecules as shown in Figure 6.

The first peak of CO_2-CO_2 RDFs in the mixture $CO_2/CH_3CH_2CH_2OH$ is broader and slightly shifted to the larger r direction than that in the mixture CO_2/CH_3OH and CO_2/C_2H_5OH, as shown in Figure 5(c). This indicates that the attractive interaction between CO_2 molecules in the mixture $CO_2/CH_3CH_2CH_2OH$ is weaker than that in the mixture CO_2/CH_3OH and CO_2/C_2H_5OH. Figure 5(d) and 5(e) show that the first peaks of the CO_2-CH_3 RDFs are higher and slightly shifted to the shorter r direction than those of CO_2-$CH_2(O)$ RDFs in the same mixtures, which suggests that CO_2 molecules interact more strongly with methyl group than methylene group of the alcohol molecules because CO_2 molecules are shielded from approaching close the methylene groups by the other sites on the same alcohol molecule.

Figure 5. Radial Distribution Functions(RDFs) in the liquid mixtures. ——— : CO_2/CH_3OH at 290 K and 2.758 MPa, ······: CO_2/C_2H_5OH at 313.14 K and 4.50 MPa, and ----: $CO_2/CH_3CH_2CH_2OH$ at 313.4 K and 4.062 MPa. $CH_2(O)$ denotes CH_2 group next to oxygen atom of alcohol molecule.

integrating RDF over the first maximum to the first minimum position. For the three alcohols in the mixtures in Figure 5, the integrals of the first peaks of the O-H RDFs and O-O RDFs yielded the coordination numbers (CNs) of the range 0.93-1.02 and 1.93-2.05, respectively. These results are consistent with the ones of pure alcohols[13,22] as well. Table 4 shows the O-H and O-O CNs for the liquid mixtures $CO_2/CH_3CH_2CH_2OH$ at 313.4 K and for different pressures. Except the mixture at 7.999 MPa, the CNs for two mixtures are similar to the ones for pure liquid $CH_3CH_2CH_2OH$. And the differences between the CNs for the mixture at 7.999

Table 4. The O-H and O-O coordination numbers (CNs) for the liquid mixtures $CO_2/CH_3CH_2CH_2OH$ at 313.4 K and for different pressures

Pressures (MPa)	O-H CNs	O-O CNs
1.171	0.94	2.01
4.062	0.95	1.99
7.999	0.84	1.79

References

1. Frenkel, D.; Mooij, G. C. A. M.; Smit, B. *J. Phys.: Condensed Matter* **1992**, *4*, 3053.
2. Laso, M.; de Pablo, J. J.; Suter, U. W. *J. Chem. Phys.* **1992**, *97*, 2817.
3. Panagiotopoulos, A. Z.; Quirke, N.; Stapleton, M.; Tildesley, D. J. *Mol. Phys.* **1988**, *63*, 527.
4. Smit, B.; Karaborni, S.; Siepmann, J. I. *J. Chem. Phys.* **1995**, *102*, 2126.
5. Siepmann, J. I.; Martin, M. G.; Mundy, C. J.; Klein, M. L. *Mol. Phys.* **1997**, *90*, 687.
6. van Leeuwen, M. E. *Mol. Phys.* **1996**, *87*, 87.
7. Martin, M. G.; Siepmann, J. I. *J. Am. Chem. Soc.* **1997**, *119*, 8921.
8. Cui, S. T.; Cochran, H. D.; Cummings, P. T. *J. Phys. Chem. B* **1999**, *103*, 4485.

9. Agrawal, R.; Wallis, E. P. *Fluid Phase Equilibria* **1997**, *131*, 51.

10. Camp, P. J.; Allen, M. P. *Mol. Phys*. **1996**, *88*, 1459.

11. Zou, M.; Lim, S. B.; Rizvi, S. S. H.; Zollweg, J. A. In *Super-critical Fluid Science and Technology*; Johnston, K. P., Penninger, J. M. L., Eds.; ACS Symposium Series No. 406, American Chemical Society: Washington, DC, 1989; Chapter 8.

12. Murthy, C. S.; Singer, K. *Mol. Phys*. **1981**, *44*, 135.

13. Jorgensen, W. L. *J. Phys. Chem*. **1986**, *90*, 1276.

14. Moon, S. D.; Moon, B. K. *Bull. Korean Chem. Soc*. **2000**, *21*, 1133.

15. Smit, B.; Siepmann, J. I. *J. Phys. Chem*. **1994**, *98*, 8442.

16. Frenkel, D.; Smit, B. *Understanding Molecular Simulation*; Academic Press: 1996.

17. Smith, W.; Fincham, D. *CCP5-Program Library*; Daresbury, UK; Science and Engineering Council: Daresbury Laboratory, 1982.

18. Hong, J. H.; Kobayashi, R. *Fluid Phase Equilibria* **1988**, *41*, 269.

19. Day, C. Y.; Chang, C. J.; Chen, C. Y. *J. Chem. Eng. Data* **1999**, *44*, 365.

20. Suzuki, K.; Sue, H.; Itou, M.; Smith, R. L.; Inomata, H.; Arai, K.; Saito, S. *J. Chem. Eng. Data* **1990**, *35*, 63.

21. Freitas, L. C. G.; Cordeiro, J. M. M.; Garbujo, F. L. L. *J. Mol. Liquids* **1999**, *79*, 1.

22. Gao, J.; Habibollazadeh, D.; Shao, L. *J. Phys. Chem*. **1995**, *99*, 16460.